

Systematic Density Functional Study of the Adsorption of Transition Metal Atoms on the MgO(001) Surface

Ilya Yudanov,^{†,§} Gianfranco Pacchioni,[‡] Konstantin Neyman,[†] and Notker Rösch^{*,†}

Lehrstuhl für Theoretische Chemie, Technische Universität München, D-85747 Garching, Germany, and Dipartimento di Chimica Inorganica, Metallorganica e Analitica, Università di Milano, via Venezian 21, 20133 Milano, Italy

Received: August 14, 1996; In Final Form: October 9, 1996[®]

We report the results of nonrelativistic and relativistic gradient-corrected density functional calculations on the interaction of single transition metal atoms with the oxygen sites of the regular MgO(001) surface. The surface has been represented by stoichiometric clusters of ions embedded in large arrays of point charges. Two adsorption sites have been considered, the on-top adsorption on the oxide anion and the bridge adsorption over two adjacent oxide anions; on-top adsorption is found to be energetically preferred. The metal atoms considered are Cr, Mo, W; Ni, Pd, Pt; Cu, Ag, and Au. These adsorbates can be classified into two groups depending on the strength of the bond with the surface. Cu, Ag, Au, Cr, and Mo exhibit weak or very weak bonds of the order of one-third of an electronvolt; their interaction is due to polarization and dispersion with little mixing with the substrate orbitals. Ni, Pd, Pt, and W, on the other hand, form relatively strong bonds, of the order of 1 eV, with the oxide anions. This bond has a covalent polar nature with little charge transfer from the metal to the oxide. This is consistent with the fact that MgO is a wide gap insulator with very weak oxidizing power. The consequences of the different bonding mechanisms for the growth of metal particles on this oxide surface are discussed.

1. Introduction

The metal–ceramic interface is of considerable technological importance in different fields such as heterogeneous catalysis, microelectronics, coating, design of magnetic devices, etc.¹ For this reason the problem has been studied quite intensively from the experimental point of view, with particular attention to potential technological applications. More recently, considerable experimental effort has been spent to better characterize the formation of metallic overlayers, emphasizing the very first stages of metal deposition.^{2–11} This intense experimental activity is complemented by a rather limited number of “first principles” theoretical studies dealing with the general problem of metal–ceramic interaction.¹² Density functional (DF) calculations have been reported on the adhesion of metal monolayers to the surface of a simple oxide like MgO.^{13–16} Hartree–Fock (HF) and DF studies have also been carried out for single metal atoms interacting with this oxide,^{17–19} and recently the first attempts to theoretically investigate the cluster deposition on oxide surfaces^{20,21} or the reactivity of surface vacancies²² have been reported. However, systematic studies of the interaction of transition metal (TM) atoms with the surface of an oxide are still lacking.

For adsorbed metal atoms, two types of interactions are usually assumed: chemical bonds (mainly with the surface oxygen atoms), on one hand, or van der Waals interaction and/or weak polarization bonds with no metalization of the surface²³ on the other. In the initial step of forming a metallic film, metal atoms impinge on the substrate. These atoms can be reflected from the surface, or they may stick to the surface, diffuse on it, and eventually reevaporate. Condensation can occur if the flux of adsorbed atoms is larger than the flux of reevaporated atoms,

and it is clear that the strength of the bond with the surface plays an essential role in this process. It should be mentioned that there is enough experimental evidence that nucleation occurs preferentially at low-coordinated defect sites, rather than on regular terraces of full-coordinated ions.⁴ Nevertheless, knowledge on how individual metal atoms interact with a regular substrate is an important prerequisite for the microscopic understanding of the nucleation and growth of supported metal particles or films.

In this paper we report for the first time a comparative investigation of the bonding of TM atoms with the oxygen ions of a regular, nondefective MgO(001) surface. The study is based on DF calculations and includes atoms from three triads of the periodic system: Cr, Mo, W; Ni, Pd, Pt; Cu, Ag, and Au. As a substrate model for investigating the adsorption on surface sites of MgO, we have used relatively large clusters of Mg and O ions embedded in an array of point charges to simulate the Madelung potential. The reliability of this comparative study is closely connected to the accuracy of the electronic structure method used. It is only in recent times that computational technology has advanced to a level that allows one to confidently predict the strength and the nature of metal–oxide bonds. Three basic prerequisites have to be met in a DF study of the above-mentioned metal adsorbates: (a) the knowledge of the response of cluster models of ionic systems like the MgO surface; (b) the inclusion of gradient corrections to the exchange–correlation energy functional to obtain reliable values of the adsorption energy; (c) the inclusion of relativistic effects for the treatment of heavy metal atoms. All these aspects are essential for a proper description of the interaction, but the last two, (b) and (c), are especially important. In fact, we have recently shown²¹ how the use of the local density approximation (LDA) leads to unreliable bond strengths for metal atoms on oxide surfaces, while the importance of relativity for the description of W, Pt, and Au atoms does not need further comments.

[†] Technische Universität München.

[‡] Università di Milano.

[§] Permanent address: Bokeskov Institute of Catalysis, Russian Academy of Sciences, 630090 Novosibirsk, Russian Federation.

[®] Abstract published in *Advance ACS Abstracts*, March 15, 1997.

In the following sections we present the results of the calculations, and we will try to draw some general conclusions about the chemical behavior of these metal atoms interacting with MgO(001). The choice of this substrate material is justified by the fact that considerable experience has been accumulated on its electronic structure and also on its interaction with adsorbates,²⁴ as well as that a variety of experimental data exists for this oxide.^{2–11}

The paper is organized as follows. In section 2 we give an outline of the theoretical method and of the basis sets and cluster models used, and we comment on the reliability of the results. Section 3 has been divided into four parts where we discuss the three triads of TM atoms adsorbed on top of oxygen, but also the possible adsorption at bridging O–O sites. In section 4 we discuss the results in view of existing experimental data and of other reported calculations, and we summarize our conclusions.

2. Computational Details

All-electron calculations were performed with the linear combination of Gaussian-type orbitals density functional (LCGTO-DF) method.²⁵ The Vosko–Wilk–Nusair local density potential was employed during the self-consistency cycles.²⁶ Finally, using the self-consistent LDA electron density, the total energy was evaluated by applying an energy functional based on the generalized gradient approximation (GGA), using the Becke exchange functional²⁷ and the Lee–Yang–Parr correlation energy functional (BLYP).²⁸ For the transition metal atoms which exhibit a very weak binding to the MgO surface (less than about 0.3 eV), one should keep in mind that the GGA does not seem to properly account for the van der Waals interaction. If the results for rare gas dimers may be generalized where a purely repulsive interaction has been calculated in GGA, then the very low binding energy values to be discussed below should be considered as lower bounds.²⁹

The scalar–relativistic version of the LCGTO-DF method was used to incorporate self-consistently the mass–velocity and Darwin relativistic corrections.^{30,31} Relativistic calculations were performed for adsorption complexes of third-row transition elements. Both nonrelativistic and relativistic calculations were carried out for systems involving second-row transition elements while only nonrelativistic calculations were done for those of first-row transition metals.

Flexible orbital basis sets were used for first,³² second,³³ and third³⁴ transition row elements, after augmentation by several *s*-, *p*-, and *d*-type diffuse exponents. The contraction scheme with $m + 2$ sets of basis functions of each angular momentum type (where m is the number of occupied shells of a given type) was chosen to yield basis sets of comparable quality for atoms belonging to different transition rows. The final bases are [15s,11p,6d/6s,5p,3d] for Cu, Ni, Cr, [18s,13p,9d/7s,6p,4d] for Ag, Pd, Mo, [21s,17p,11d,7f/8s,7p,5d,3f] for Au, and [21s,17p,12d,7f/8s,7p,5d,3f] for Pt and W. Special care was taken when choosing the diffuse *d* exponents of the second-row transition elements. For instance, addition of one diffuse *d* exponent to the [18s,13p,8d] basis set³³ of Ag and Mo causes significant changes in the bond lengths of test diatomics. The basis sets for Mg and O used previously³⁵ were extended and modified to minimize the basis set superposition error (BSSE).³⁶ The complete basis sets are [15s,10p,1d/6s,5p,1d] for Mg and [13s,8p,1d/6s,5p,1d] for O. All contractions were of the general type, based on appropriate nonrelativistic or relativistic LDA atomic eigenvectors. The BSSE was taken into account by means of the standard Boys–Bernardi correction.³⁶

The fitting basis sets used in the LCGTO-DF method to represent the electron charge density and the exchange–correla-

TABLE 1: Selected Excitation Energies (in eV) for High-Spin Configurations of Various Transition Metal Atoms

	configuration		excitation energy	
	ground state	excited state	calc ^a	exp ^b
Cr	3d ⁵ 4s ¹	3d ⁴ 4s ²	1.45	1.00
Mo	4d ⁵ 5s ¹	4d ⁴ 5s ²	1.65	1.47
W	5d ⁵ 6s ¹	5d ⁴ 6s ²	0.09	0.18
Ni	3d ⁹ 4s ¹	3d ¹⁰	1.52	1.74
	3d ⁹ 4s ¹	3d ⁸ 4s ²	1.01	0.58
Pd	4d ¹⁰	4d ⁹ 5s ¹	0.98	0.95
Pt	5d ⁹ 6s ¹	5d ¹⁰	0.51	0.72
Cu	3d ¹⁰ 4s ¹	3d ⁹ 4s ²	1.75	1.49
Ag	4d ¹⁰ 5s ¹	4d ⁹ 5s ²	3.91	3.97
Au	5d ¹⁰ 6s ¹	5d ⁹ 6s ²	1.65	1.74

^a Relativistic calculation. ^b Experimental values are obtained from ref 42 by averaging over individual states where appropriate.

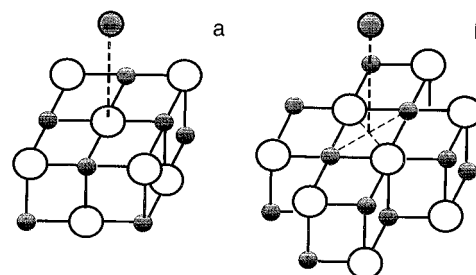


Figure 1. M–O₉Mg₉ and M–Mg₁₂O₁₂ cluster models of on-top and bridge sites at the MgO(001) surface. White, black, and dotted circles represent oxygen, magnesium, and adsorbed metal atoms, respectively.

tion potential during the self-consistency cycles were constructed in a standard fashion.²⁵ For the “post-SCF” evaluation of the total energy, the exchange–correlation contribution was calculated using an accurate numerical integration procedure.³⁷

An important aspect of the interaction of TM atoms with MgO, as will be discussed below, is the ability of the metal to form *s*–*d_σ* hybrid orbitals for improved mixing with the *s*–*p* orbitals of the surface oxygen anions. For this reason the energy separation between atomic configurations with different *s* and *d* occupations is a particularly important atomic property. In Table 1 we compare the energy separations between some low-lying atomic states computed at the relativistic level with the corresponding experimental values. The agreement between theoretical and measured energy separations can be considered as satisfactory.

The MgO(001) surface was modeled by two-layer molecular clusters (Figure 1): the oxygen-centered cluster O₉Mg₉ (*C*_{4v} point group) and the cluster Mg₁₂O₁₂ (*C*_{2v}). The O₉Mg₉ cluster was used to represent on-top adsorption of metal atoms on the central oxygen ion. The Mg₁₂O₁₂ cluster was employed for modeling adsorption at the bridge position. To simulate the Madelung field of the surrounding ions, the clusters were embedded into arrays of point charges with the dimensions 17 × 17 × 6 and 16 × 16 × 6 for O₉Mg₉ and Mg₁₂O₁₂, respectively. For these charges the value for the ideal ionic crystal, ±2.0 au, has been assumed. The Mg–O distance for clusters and for surrounding point charges was taken from the experimental MgO bulk geometry (3.976 au).

For each adsorbed metal atom several points at different distances from the surface were calculated. The potential curves, not corrected for the BSSE, were fitted by a polynomial to calculate the equilibrium geometry as well as the corresponding force constants and vibrational frequencies. The vibrational frequency $\omega_e(\text{O}–\text{M})$ of the M–O mode was calculated under the assumption of a rigid substrate of infinite mass. To avoid the limitations of a Mulliken population analysis, in particular in connection with diffuse basis functions as used in the present

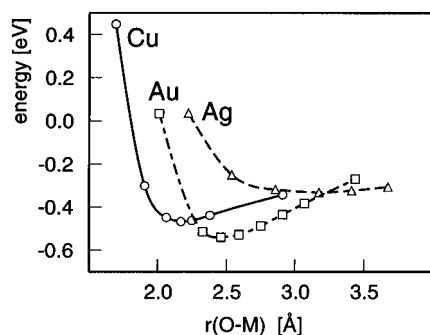


Figure 2. Potential energy curves for the 2A_1 states of Cu (O), Ag (Δ), and Au (\square) atoms interacting with a surface oxygen of MgO: Cu, nonrelativistic calculation; Ag and Au, relativistic calculations.

TABLE 2: Calculated Adsorption Properties of Cu, Ag, and Au Atoms on MgO(001)

state	Cu(2A_1) nonrel	Ag(2A_1)		Au(2A_1) rel
		nonrel	rel	
$r_e(\text{O-M}),^a \text{ \AA}$	2.18	3.29	3.17	2.47
$\omega_e(\text{O-M}),^b \text{ cm}^{-1}$	98	29	28	52
$f(\text{O-M}),^c \text{ mdyn/\AA}$	0.36	0.05	0.05	0.32
$D_e,^d \text{ eV}$	0.47	0.40	0.33	0.54
$D_e \text{ (BSSE)},^e \text{ eV}$	0.30	0.28	0.20	0.23
$d\mu/dr,^f \text{ au}$	0.24	0.34	0.25	0.31

^a O-M bond equilibrium bond distance. ^b Frequency of the O-M stretching mode. ^c Corresponding force constant. ^d Adsorption energy. ^e BSSE-corrected adsorption energy. ^f Dynamic dipole moment of the O-M motion at equilibrium geometry.

case, the charge transfer from the adsorbed metal to the surface was estimated with the help of the dynamic dipole moment associated with the surface-metal atom stretching mode.^{38,39}

3. Results

3.1. Cu, Ag, Au. The valence electronic structure of Cu, Ag, and Au atoms is characterized by the presence of a filled d shell and a singly occupied s orbital. This prevents the atoms from easily changing their configuration during bond formation. The lowest-lying excited state, d^9s^2 , is in fact ≈ 1.7 eV higher than the ground state for Cu and Au and about 4 eV higher for Ag; see Table 1. On the other hand, Cu, Ag, and Au could, in principle, form relatively strong bonds with oxygen atoms of not fully reduced oxide surfaces by partial transfer of their outer electron to the substrate.

The potential energy curves for the 2A_1 states are shown in Figure 2 while the corresponding adsorption properties are given in Table 2. For Ag we report the results of both relativistic and nonrelativistic calculations. The first observation from the orbital analysis is that the adsorbed atoms retain their $nd^{10}(n+1)s^1$ atomic character. However, a very small mixing of the metal σ orbitals with the O $2p_\sigma$ orbital is also found. All atoms are weakly bound to the surface. The dissociation energy, corrected for the BSSE, goes from 0.30 eV for Cu to 0.20 and 0.23 eV for Ag and Au, respectively. The weak bonding is shown also by the very low values of the frustrated translation, perpendicular to the surface, which is characterized by a vibrational frequency of 100 cm^{-1} and smaller. Actually, the curve for Ag is extremely shallow, with a bond length of about 3.2 Å and a vibrational frequency ω_e of only 28 cm^{-1} (Table 2). In such cases of very weak adsorption these observables, to a certain degree, depend on the exchange-correlation potential used. Employing a Becke-Perdew^{27,40} (BP) potential in a relativistic calculation for Ag on MgO, we found an adsorption height of 2.6 Å and a BSSE-corrected adsorption energy of 0.3 eV. However, the large change in surface-Ag distance is not too surprising if one takes into account that the potential energy

TABLE 3: Calculated Adsorption Properties^a of Ni, Pd, and Pt Atoms on MgO(001)

	Ni(1A_1)		Ni(3B_2)		Pd(1A_1)		Pt(1A_1)		Pt(3B_2)	
	state	nonrel	nonrel	nonrel	rel	rel	rel	rel	rel	rel
$r_e(\text{O-M}), \text{ \AA}$		1.87	2.22	2.28	2.15	2.00	2.37			
$\omega_e(\text{O-M}), \text{ cm}^{-1}$		249	107	101	134	160	75			
$f(\text{O-M}), \text{ mdyn/\AA}$		2.12	0.39	0.65	1.14	2.95	0.65			
$D_e, \text{ eV}$		0.99	0.52	0.63	0.95	1.85	0.94			
$D_e \text{ (BSSE)}, \text{ eV}$		0.88	0.41	0.49	0.81	1.36	0.49			
$d\mu/dr, \text{ au}$		0.48	0.16	0.04	0.10	0.16	0.11			

^a For the designation of the various properties, see Table 2.

curve is very shallow even at the BP level (ω_e is 90 cm^{-1}); under these conditions, a small change in the potential entails a large change in the distance. More importantly, the nature of the bonding is exactly the same, no matter which exchange-correlation potential is used.

Some information on the occurrence of charge transfer from the adsorbate to the surface can be obtained from the analysis of the dipole moment curve for the vertical motion of the adsorbate.³⁸ This is particularly the case for ionically bound adsorbates, where the dipole moment curve exhibits a linear behavior and a large slope. In fact, for an ionic adsorbate with a charge q and in the absence of any intraunit polarization, the dipole moment curve $\mu(r) = q(r - r_e) + \mu_0$ is a linear function of the adsorption height r , resulting in a constant dynamic dipole moment $d\mu(r)/dr = q$. For a covalent adsorbate, on the other hand, the $d\mu/dr$ curve exhibits a small slope and a pronounced curvature.³⁸ The $d\mu/dr$ curves for Au, Cu, and Ag are similar, exhibiting a nonlinear behavior with small slopes (Table 2). Both these characteristics exclude the occurrence of a substantial charge transfer from the metal atom to the substrate. The bonding can thus be described as mainly due to the polarization of the metal electrons by the surface electric field, accompanied by a relatively modest chemical interaction. The polarization contribution to the bonding can be estimated by placing a neutral atom at a fixed distance from a distribution of point charges simulating the ionic MgO(001) surface. For Cu at 4.2 au from the surface, a stabilization of 1.1 eV results. This attractive term, however, is partially compensated by the Pauli repulsion with the surface electron density, such that the final bond is rather weak. This result suggests that the oxide anions of the MgO surface are highly charged, with little tendency to ionize the adsorbed coinage atoms. The relatively weak bonding found for Cu, Ag, and Au is therefore a consequence of the large adatom size (due to the singly occupied valence s orbital) which determines the long surface-adsorbate distance. Ag behaves somewhat differently from Cu and Au: the bond distance is even longer than for the other two members of the triad. This difference may be related to the large energy separation between the Ag 4d and 5s levels compared to the d-s separation in Cu and Au which is reflected in the very different $s^1d^{10} \rightarrow s^2d^9$ transition energies (Table 1). The smaller propensity for a metal s-d hybridization and for a mixing with the oxygen levels is most likely the reason for the weaker bonding of Ag.

3.2. Ni, Pd, Pt. The interaction of Ni, Pd, and Pt atoms with MgO is considerably more complex than that of the coinage metal atoms. The main reason for this difference is the interplay between the d^{10} , the d^9s^1 , and, at least for Ni, the d^8s^2 configurations of the atoms. The interaction of free atoms with the MgO cluster gives rise to several states; we have investigated the low-lying triplets and the lowest closed-shell singlet. The lowest triplet and singlet states, 3B_2 and 1A_1 , correlate at infinite separation with $\text{MgO} + \text{M}(d^9s^1)$ and $\text{MgO} + \text{M}(d^{10})$, respectively; see Table 3. For Pd, however, only the 1A_1 state was considered as this is the state which correctly dissociates into ground state fragments. The 3B_2 curves for Ni and Pt surface

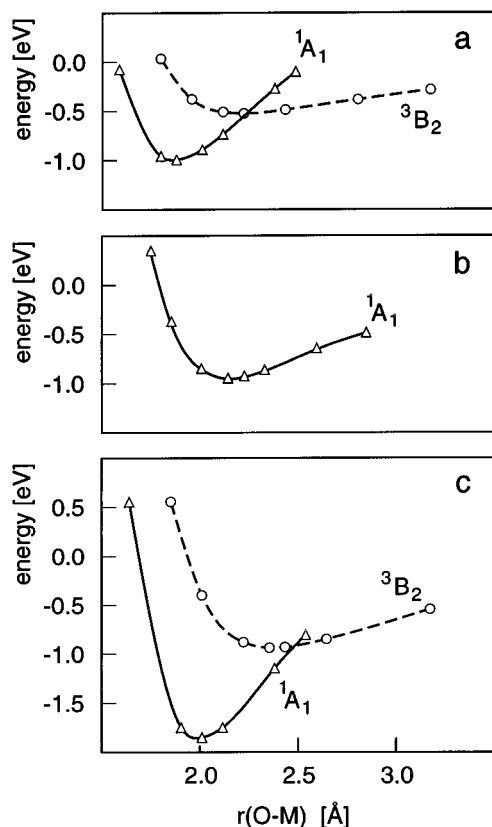


Figure 3. Potential energy curves for the 3B_2 (O) and 1A_1 (Δ) states of (a) Ni, (b) Pd, and (c) Pt atoms interacting with a surface oxygen of MgO: Ni, nonrelativistic calculation; Pd and Pt, relativistic calculations.

complexes exhibit rather shallow minima (at about 2.2 and 2.4 Å) and a relatively weak bonding (0.5 eV for Ni and 0.9 eV for Pt before BSSE correction, Table 3). The state 3B_2 features the lowest energy for long surface-metal distances. At shorter distances, however, a crossing of the 3B_2 with the 1A_1 state occurs (Figure 3). Below about 2.2 Å (for Ni) or 2.5 Å (for Pt) the 1A_1 becomes the ground state; the potential energy curve exhibits a deeper minimum and a rather high adsorption energy of about 1 eV or more, depending on the metal (see Table 3).

The curve crossing implies that a magnetic quenching accompanies the formation of the bond. This is reminiscent of the bonding mechanism of CO ligands on Ni atoms, clusters, or surfaces.⁴¹ In this case the overlap of the CO charge density with the diffuse Ni 4s orbital results in a repulsive interaction that is partially reduced by promoting the 4s electron into the 3d shell with consequent spin quenching. The interaction with the MgO surface, however, is somewhat different. Here the key mechanism for the bonding is the formation of s-d hybrid orbitals which is able to conveniently mix with the O $2p_\sigma$ orbitals; in fact, in the 1A_1 configuration the metal s, d_σ , and the O $2p_\sigma$ orbitals are strongly hybridized. The low-spin coupling of the metal open-shell electrons seems to favor the bonding with the surface oxygen; a possible explanation for the Ni, Pd, and Pt triad is that in the 1A_1 state the mixing with the d^{10} configuration, which generates only this state, decreases the repulsion of the metal ($n+1$)s electron with the surface with subsequent reduction of the metal-oxygen distance.

At the 1A_1 equilibrium distance Ni, Pd, and Pt form rather strong chemical bonds with the surface. The trend of the binding energies is Pt > Ni \approx Pd (Table 3). Pt features also the largest force constant, followed by Ni and Pd. Thus, Pd is somewhat special in the triad, with the longer distance, the weaker bonding, and the smallest force constant. This is true even after introduction of relativistic effects which turn out to

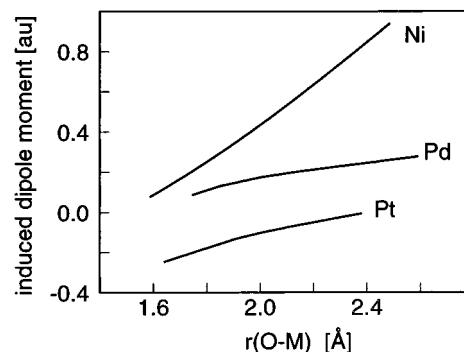


Figure 4. Induced dipole moment curves for the vertical displacement of Ni, Pd, and Pt on MgO (1A_1 state).

be rather important for the proper description of the adsorption properties; see Table 3.

The dipole moment curves reveal a significant difference between Ni on one side and Pd and Pt on the other (Figure 4). Ni exhibits an almost linear curve with a relatively large slope of 0.48 au, indicative of a nonnegligible polarity of the bond with MgO. Pd and Pt, on the other hand, feature dipole moment curves with small slopes and large curvatures (Figure 4). This seems to indicate a more covalent character of the interaction between Pd and Pt orbitals and the oxygen 2p orbitals. A possible explanation of this difference comes from the values of the Ni, Pd, and Pt ionization potentials. We used here the nd^{10} state as a reference, but the trends are similar for other electronic configurations. Ni has the lowest computed ionization energy $d^{10} \rightarrow d^9$, 6.81 eV (experiment, 5.88 eV),⁴² while Pd and Pt show larger, comparable ionization potentials, 8.91 and 9.06 eV, respectively; the corresponding experimental values are 8.51 and 8.62 eV.⁴² The fact that Ni is easier to ionize is in agreement with the largest slope of the dipole moment curve and with a more polar bond.

However, we would like to stress that the bonding can by no means be viewed simply as a charge transfer from the metal atom to the oxide surface. The orbital analysis clearly shows a substantial mixing (hybridization) of metal nd and O $2p$ orbitals. This mixing leads to a covalent bond with some polar character for Ni and little polarity for Pd and Pt. The fact that all three atoms in the group form relatively strong bonds with the surface, compared for instance to the coinage metals, can be explained with the more pronounced tendency of the group 10 atoms to form s-d hybrid orbitals and a more direct involvement of the d orbitals in the bond with the oxygen. This tendency can be generally related to the $s \rightarrow d$ (or $d \rightarrow s$) transition energies; the computed $d^9s^1-d^{10}$ energy separations in Pd and Pt, 0.51 and 0.98 eV, respectively, are considerably lower than the $d^{10}s^1 \rightarrow d^9s^2$ transition energy in Cu or Au, about 1.7 eV. In Ni, the $d^9s^1 \rightarrow d^{10}$ transition occurs at 1.52 eV, but s-d mixing is favored by the fact that the d^8s^2 configuration is close to the d^9s^1 (Table 1).

3.3. Cr, Mo, W. The interplay between high-spin and low-spin states plays a significant role in the interaction of Cr, Mo, and W atoms with MgO. These atoms have high-spin atomic ground states $nd^5(n+1)s^1$ (7A_1 in C_{4v} symmetry); their d shell is therefore half-filled, and a comparison of their interaction with that of the late TM atoms will be particularly instructive. Low-spin, quintet, states have also been considered. Triplet states have been studied, but their energy is considerably higher, and they will not be further discussed.

At long surface-Cr distances the ground state for the cluster is 7A_1 , which correctly dissociates into Cr and MgO ground states. This state exhibits a very shallow potential energy curve, with a minimum around 2.8 Å and a binding energy of 0.34 eV (BSSE corrected) (Figure 5 and Table 4). The flat nature

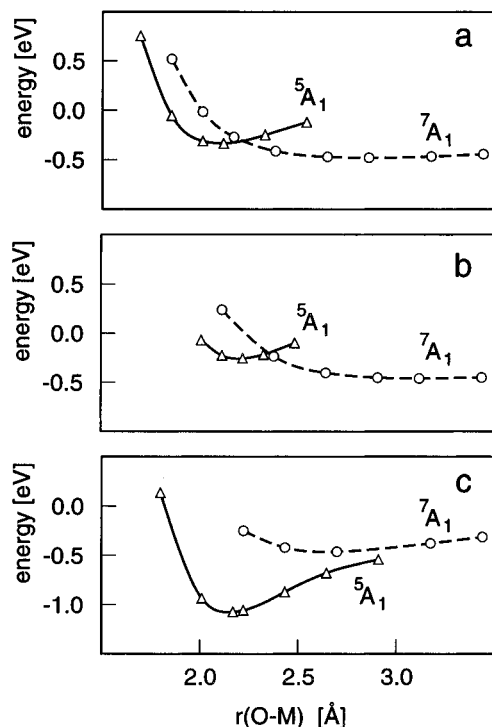


Figure 5. Potential energy curves for the 7A_1 (O) and 5A_1 (Δ) states of (a) Cr, (b) Mo, and (c) W atoms interacting with a surface oxygen of MgO: Cr, nonrelativistic calculation; Mo and W, relativistic calculations.

TABLE 4: Calculated Adsorption Properties^a of Cr, Mo, and W Atoms of Mg(001)

state	Cr(7A_1) nonrel	Mo(7A_1)		W(5A_1) rel
		nonrel	rel	
$r_e(\text{O-M})$, Å	2.83	3.33	3.14	2.16
$\omega_e(\text{O-M})$, cm^{-1}	48	25	29	117
$f(\text{O-M})$, $\text{mdyn}/\text{\AA}$	0.07	0.04	0.05	1.47
D_e , eV	0.48	0.51	0.46	1.07
D_e (BSSE), eV	0.34	0.39	0.33	0.72
$d\mu/dr$, au	0.16	0.33	0.16	0.71

^a For the designation of the various properties, see Table 2.

of the curve is shown by the very low values of the force constant and of the vibrational frequency, 48 cm^{-1} . At distances shorter than 2.2 \AA , however, the 5A_1 low-spin state becomes lower in energy. This second state has a shorter equilibrium distance and a larger force constant, but its total equilibrium energy is slightly higher than that of the high-spin state (Figure 5). The same behavior is found for Mo. In fact, also in this latter case the 7A_1 state is lowest in energy, with an equilibrium distance at large separation from the surface, close to 3 \AA , and a binding energy of 0.33 eV ; the force constant is even smaller than for Cr (Table 5). Below 2.3 \AA the low-spin 5A_1 state becomes energetically preferred (Figure 5), but again with an equilibrium energy slightly higher than for the 7A_1 state. The two atoms, Cr and Mo, also have similar dipole moment curves, with very small slopes and pronounced curvatures. Given the shape of the potential curve for the 7A_1 state, it is possible to conclude that the bonding is largely due to polarization and dispersion, with little, if any, chemical mixing of the metal orbitals with the surface electronic states. In the 5A_1 state the nd_{z^2} and $(n+1)s$ atomic orbitals are strongly hybridized. The hybridization reduces the spatial extent of the outer s orbital, hence the repulsion with the surface, and ultimately leads to a shorter equilibrium distance. Nevertheless, the degree of mixing of the metal orbitals with the surface oxygen orbitals remains quite low, and the interaction is still very weak.

TABLE 5: Calculated Adsorption Properties^a of Cu and Ni Atoms at the Bridge Position on Mg(001)

state	Cu(2A_1) nonrel	Ni(FON ^b) nonrel
$r_e(\text{O-M})$, Å	2.84	2.47
$\omega_e(\text{O-M})$, cm^{-1}	76	136
$f(\text{O-M})$, $\text{mdyn}/\text{\AA}$	0.22	0.61
D_e , eV	0.68	0.43
D_e (BSSE), eV	0.21	0.02
$d\mu/dr$, au	0.22	0.23

^a For the designation of the various properties, see Table 2. ^b Not a pure spin state, but calculated using the fractional occupation number (FON) technique.²⁵

A completely different bonding arises from the interaction of W with MgO. The interaction of W in the high-spin d^5s^1 configuration results in a flat curve, very similar to those computed for Cr and Mo (Figure 5). This state, however, is not the ground state, even for long surface-adsorbate distances. On the other hand, the low-spin 5A_1 state exhibits a deep minimum near 2.15 \AA ; in this minimum, W is bound to MgO by 0.72 eV (BSSE corrected value). This is a substantial chemical bond of similar strength than that calculated for the Ni triad. A population analysis shows that in this state the d^4s^2 atomic configuration is mixed not only with the d^5s^1 state but also with the O $2p$ orbitals. This is consistent with the fact that the s - d transition energy is smallest in W where the s^1d^5 and the s^2d^4 states are almost isoenergetic, in contrast to the situation for Cr and Mo (Table 1). The easy s - d hybridization is actually the reason for the strong bonding of W. As for adsorbed Ni, the bond with W exhibits a considerable polar character, as shown by a rather linear dipole moment curve with its large slope, 0.71 au (Table 4).

3.4. Adsorption at Bridge Sites. So far we have considered the interaction of isolated metal atoms on top the oxygen anions at the terraces of the MgO(001) surface. Of course, other adsorption sites are possible, like the Mg ions or the bridge sites (Mg-Mg, Mg-O, or O-O bridge sites). Previous studies based on both DF²¹ or HF²² methods have clearly shown that the interaction of metal atoms with the surface cations is rather weak and due to polarization effects. Chemical arguments also suggest that the only possible strong interaction must involve the surface oxygen anions.

In this section we investigate the possible bonding of metal atoms at the O-O bridging sites of the MgO(001) surface. As examples, we have studied adsorption of only the Cu and Ni atoms. The results are summarized in Table 5. On an O-O bridge site Cu is bound by 0.21 eV , but the O-Cu distance has increased from 2.18 (on-top) to 2.84 \AA (bridge). For Ni the change is even more dramatic, but in the same direction. The O-Ni distance increases by 0.6 \AA , and the binding energy decreases from 0.9 eV to almost zero (Table 5).

The first conclusion from these data is that the bridge site is less stable than the on-top one. This confirms previous calculations of the same quality on the deposition of small Ni and Cu clusters on MgO(001).²¹ Furthermore, while the change in bond strength for Cu is relatively small, from 0.3 to 0.2 eV , the change is much larger for Ni, which becomes virtually unbound. This provides additional evidence for the different nature of the bonding in the two cases. The Cu orbitals mix relatively little with the O $2p$ band, and the bonding is partly due to polarization effects; this finding implies that small changes in the bond strength are expected for different surface positions of the adsorbate. For Cu, the best adsorption site will largely be determined by the electrostatic potential of the ionic surface. On the other hand, Ni is bound to the surface through a covalent polar bond. Covalent bonds are highly directional,

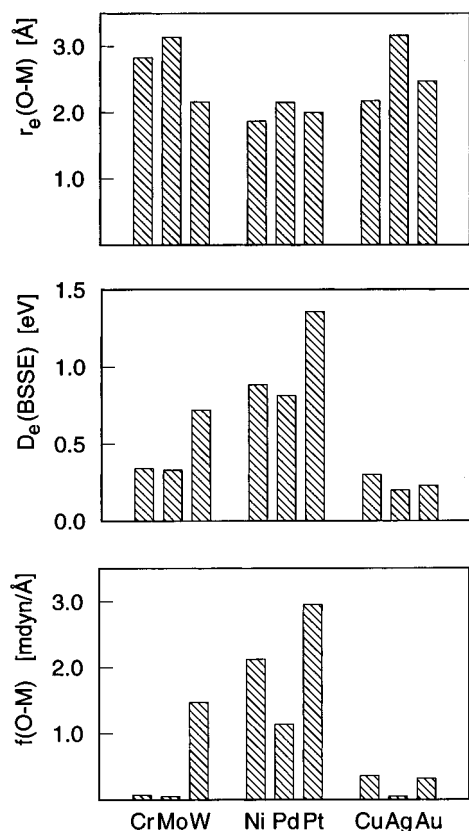


Figure 6. Trends in bond lengths $r_e(\text{O-M})$, adsorption energies $D_e(\text{BSSE})$, and force constants $f(\text{O-M})$ of Cr, Mn, W, Ni, Pd, Pt, Cu, Ag, and Au interacting with a surface oxygen of MgO.

and the displacement of the atom from the on-top position results in a strong destabilization. This may have consequences for the barriers to diffusion of the metal atoms on the surface.

4. Discussion and Conclusions

The trends in bond lengths, force constants, and adsorption energies for the TM atoms considered in this work are shown in Figure 6. It is apparent that the Ni, Pd, and Pt triad is the only one for which strong interface bonds are formed. The adhesion energy of these atoms on top of surface oxygens is about 1 eV/atom or more. The only other metal atom considered in this work that exhibits a tendency to form strong bonds with the surface is W. For W, in fact, we computed a bond strength and a force constant comparable to those of the Ni triad. This tendency to form strong bonds is connected with the fact that metal s and d orbitals hybridize and that these hybrid orbitals mix with the p orbitals of the surface oxygen. Pd is somewhat special in the Ni triad as it has the smallest binding energy and the longest distance from the surface. This reflects the general tendency toward a nonmonotonous behavior in many chemical properties as one moves down a TM group; in particular, second-row TM atoms often exhibit weaker interactions than the isovalent first- and third-row atoms.^{43,44} To some extent, this trend is observed also for the triad Cr, Mo, and W as well as for the triad Cu, Ag, and Au (see Figure 6). The bonding of Cr, Mo, Cu, Ag, and Au to a MgO substrate, however, can be classified as weak, arising mainly from polarization and dispersion effects with only minor orbital mixing with the surface oxygen orbitals. This explains the very long bond distances found in some cases and the flat potential energy curves which result in very small force constants.

Thus, the TM atoms considered can be classified into two groups: atoms that tend to form relatively strong chemical bonds with the surface oxygen anions of MgO (Ni, Pd, Pt, and W)

and atoms that interact very weakly with the surface, with adsorption energies of the order of one-third of an electronvolt or less (Cr, Mo, Cu, Ag, and Au). In the first case the bonding originates from the direct mixing of the metal d orbitals with the surface O 2p band. This interaction is covalent in nature and *does not imply a significant charge transfer from the metal to the surface*. This is an important conclusion. It is connected to the highly ionic nature of the MgO surface where the surface oxygen atoms have their valence almost saturated. To a first-order approximation, MgO can be described in terms of classical ionic model, $\text{Mg}^{2+}-\text{O}^{2-}$; however, a more realistic estimate on the charge separation according to slab LDA calculations is that the Madelung field outside the surface is comparable to that of an array of point charges with ± 1.8 au.⁴⁵ This means that the oxygen centers at the *regular surface sites of MgO(001)* are almost completely reduced and are not able to oxidize the adsorbed metal atoms. This is different from other oxides, e.g. TiO_2 , where the partial ionic nature of the surface results in a strong oxidizing power of the surface oxygens⁴⁶ or from other surface sites of MgO, in particular oxygen and magnesium vacancies, the F and V centers, where a completely different chemistry occurs.²²

The fact that the interfacial bond has a substantially covalent polar character explains why no correlation is found between the computed adsorption energies and the enthalpies of formation of the bulk oxides, $\Delta H_{\text{for}}^\circ$. A correlation between the adhesion energy and the oxide enthalpy of formation has been proposed⁴⁷ to explain the different growth mechanism of metal clusters or films on oxide surfaces (on TiO_2 , in particular). However, no correlation is found in the present case. Take the Cr triad as an example: the values of $\Delta H_{\text{for}}^\circ$ for the binary oxides CrO_2 , MoO_2 , and WO_2 are -598.0 , -588.9 , and -589.7 kcal/mol, respectively.⁴⁸ Clearly, no relation exists with the computed adsorption energies for the isolated Cr, Mo, and W atoms on MgO. This difference in behavior may be rationalized by the fact that while metal atoms in the bulk oxides are significantly oxidized, this is not the case for the single atoms on the MgO(001) surface.

Very few ab initio studies on the metal–oxide interface have been reported so far. Usually two approaches have been considered: band structure calculations on the adhesion of a full metal monolayer on oxide substrate (MgO is the most widely studied) or cluster calculations on the interaction between isolated metal atoms or clusters and the oxide. In a pioneering work, Kunz et al. have considered the adsorption of Cu and Ni atoms on the surface of MgO ^{17,18} and Al_2O_3 ⁴⁹ using the HF method. For MgO they found a very weak bonding with a surface oxygen (0.04 eV) at a distance of about 4 Å. Clearly, this is not a true bond, and it is likely to disappear if the BSSE is taken into account. A similar weak or repulsive interaction has recently been found at the HF level for Rb, Pd, or Ag atoms interacting with the surface O ions of MgO.²² All these results which suggest the MgO(001) surface to be quite unreactive toward these metal atoms are at variance with a recent LDA study of the interaction of a Cu atom with MgO.¹⁹ In this work, in fact, a strong bond of 1.42 eV was reported for a relatively short O–Cu distance, 1.96 Å. Thus, a contradicting picture emerges: the present GGA-based DF work and the HF calculations indicate that Cu and Ag atoms are only weakly bound to MgO while the LDA calculations predict a strong bond. This discrepancy was recently solved by work done in our group.²¹ We have shown that the LDA result is incorrect and that the large binding disappears when density gradient corrections to the exchange–correlation energy functional are taken into account (as also done in the present investigation); in this latter case the bonding of Cu is of about 0.3 eV (Table

2).²¹ To the best of our knowledge, no other "first principles" studies of the interaction of metal atoms with MgO have been reported. However, it should be mentioned that a HF study of the interaction with surface vacancies of MgO has shown the extremely important role of these defects in the early stages of the metal-oxide deposition.²²

When deposition of metal films is considered, a comparison between the present adsorption energies and the computed adhesion energies in the monolayer regime is possible. Li et al.¹⁵ have studied an Ag monolayer on MgO by means of the full-potential linearized augmented-plane-wave method. They found an adhesion energy of 0.54 J/m² corresponding to an adsorption of 0.3 eV/atom, close to our computed value. A slightly larger bond strength was reported by Smith et al.¹⁶ who found an adhesion of 0.95 J/m² or 0.53 eV/atom. In this respect, the relatively high interfacial bond, 0.9 eV/atom, reported by Schönberger et al.¹³ for bulk fcc Ag on MgO(001) is probably due to the use of the local density approximation. A somewhat stronger bond between an Ag monolayer and CdO, 0.63 eV/atom, was recently reported by Rao et al.⁵⁰ As for Ag/MgO, the bonding was found to imply no charge transfer between the metal and the substrate. The same has been found for other metal films, Fe in particular, deposited on MgO.¹⁴

From the experimental point of view, very little is known about the interaction of isolated metal atoms. The studies of Zhou et al.⁶ and of Wu et al.⁷ where the initial sticking probability of Cu atoms on MgO has been measured are particularly relevant to the present work. Zhou et al.⁶ found that on a clean surface only 50% of the initially incident Cu atoms stick to the surface at 300 K, and they estimated a desorption energy of 0.2–0.5 eV. Wu et al.⁷ found a higher value of the sticking probability, 0.8. This value is still below 1, indicative for a moderately strong interaction with the substrate. These experiments are in qualitative agreement with the present calculations.

Finally, we discuss the relevance of the present results for the growth mechanism of metals on MgO. The first observation is that none of the MgO/metal bonds considered are very strong and that Cu, Ag, and Au are among the atoms which form the weakest bonds. This is consistent with the idea that the adhesion energy at the metal-oxide interface is smallest for wide-gap insulators, as MgO, and for metals featuring a small conduction electron density, like Cu or Ag. It is generally assumed¹ that strong metal-oxygen bonds favor metal spreading with layer-by-layer growth (Franck-van der Merwe mechanism) while weak adsorbate-substrate interactions result in three-dimensional cluster growth (Volmer-Weber mechanism). For MgO(001), all the computed adsorption energies, even those of Ni, Pd, Pt, and W, are considerably smaller than the metal-metal bond strength in the corresponding clusters or bulk metals.⁴⁸ This leads to the conclusion that clustering should be preferred during metal deposition on MgO. This has indeed been observed for Pd and Ag on MgO.^{9–11} However, it should be noted that the presence of impurities plays a crucial role in the dynamics of the deposition and that completely different growth modes have been observed for Ag deposited on clean and defective MgO surfaces.⁸ Clearly, further theoretical work on the interaction of transition metal atoms with surface defects of ionic substrates is highly desirable.

Acknowledgment. This work has been supported by the INTAS program of the European Community, Grant 93-1876-

ext. G.P. and I.Y. thank the "Vigoni Program" from CRUI and DAAD for supporting their visits to the Technical University of Munich and to the University of Milano, respectively. The work of the Munich group is supported by the Deutsche Forschungsgemeinschaft, Bayerischer Forschungsbund Katalyse (FORKAT), and Fonds der Chemischen Industrie.

References and Notes

- (1) Rühle, M.; Evans, A. G.; Ashby, M. F.; Hizth, J. P., Eds. *Metal-Ceramic Interfaces*; Pergamon: Oxford, 1990.
- (2) He, J.-W.; Möller, P. J. *Surf. Sci.* **1987**, *180*, 411.
- (3) He, J.-W.; Möller, P. J. *Surf. Sci.* **1986**, *178*, 934.
- (4) He, J.-W.; Möller, P. J. *Chem. Phys. Lett.* **1986**, *129*, 13.
- (5) Alstrup I.; Möller, P. J. *Appl. Surf. Sci.* **1988**, *33/34*, 143.
- (6) Zhou, J. B.; Lu, H. C.; Gustafsson, T.; Garfunkel, E. *Surf. Sci.* **1993**, *293*, L887.
- (7) Wu, M.-C.; Oh, W. S.; Goodman, D. W. *Surf. Sci.* **1995**, *330*, 61.
- (8) Didier, F.; Jupille, J. *Surf. Sci.* **1994**, *307–309*, 587.
- (9) Meunier, M.; Henry, C. R. *Surf. Sci.* **1994**, *307–309*, 514.
- (10) Henry, C. R.; Meunier, M.; Morel, S. J. *Cryst. Growth* **1993**, *129*, 416.
- (11) Kizuka, T.; Kachi, T.; Tanaka, N. Z. *Phys. D* **1993**, *26*, S58.
- (12) Noguera, C.; Bordier, G. J. *Phys. III* **1994**, *4*, 1851.
- (13) Schönberger, U.; Andersen, O. K.; Methfessel, M. *Acta Metall. Mater.* **1992**, *40*, S1.
- (14) Li, C.; Freeman, A. J. *Phys. Rev. B* **1991**, *43*, 780.
- (15) Li, C.; Wu, R.; Freeman, A. J.; Fu, C. L. *Phys. Rev. B* **1993**, *48*, 8317.
- (16) Smith, J. R.; Hong, T.; Srolovitz, D. J. *Phys. Rev. Lett.* **1994**, *72*, 25.
- (17) Bacalis, N. C.; Kunz, A. B. *Phys. Rev. B* **1985**, *32*, 4857.
- (18) Kunz, A. B. *Philos. Mag. B* **1985**, *51*, 209.
- (19) Li, Y.; Langreth, D. C.; Pederson, M. R. *Phys. Rev. B* **1995**, *52*, 6067.
- (20) Pacchioni, G.; Röscher, N. *Surf. Sci.* **1994**, *306*, 169.
- (21) Pacchioni, G.; Röscher, N. *J. Chem. Phys.* **1996**, *104*, 7329.
- (22) Ferrari, A. M.; Pacchioni, G. J. *Phys. Chem.* **1996**, *100*, 9032.
- (23) Gautier, M.; Duraud, J. P. J. *Phys. III* **1994**, *4*, 1779.
- (24) Neyman, K. M.; Pacchioni, G.; Röscher, N. In *Recent Developments and Applications of Modern Density Functional Theory*; Seminario, J. M., Ed.; Elsevier: Amsterdam, 1996; p 569.
- (25) Dunlap, B. I.; Röscher, N. *Adv. Quantum Chem.* **1990**, *21*, 317.
- (26) Vosko, S. H.; Wilk, L.; Nusair, M. *Can. J. Phys.* **1980**, *58*, 1200.
- (27) Becke, A. D. *Phys. Rev. A* **1988**, *38*, 3098.
- (28) Lee, C.; Yang, W.; Parr, R. G. *Phys. Rev. B* **1988**, *37*, 785.
- (29) Pérez-Jordá, J. M.; Becke, A. D. *Chem. Phys. Lett.* **1995**, *233*, 134.
- (30) Häberlen, O. D.; Röscher, N. *Chem. Phys. Lett.* **1992**, *199*, 491.
- (31) Häberlen, O. D.; Chung, S.-C.; Röscher, N. *Int. J. Quantum Chem. Quantum Chem. Symp.* **1994**, *28*, 595.
- (32) Wachters, A. J. H. J. *Chem. Phys.* **1970**, *52*, 1033.
- (33) Huzinaga, S. J. *Chem. Phys.* **1977**, *66*, 4245.
- (34) Gropen, O. J. *Comput. Chem.* **1987**, *8*, 982.
- (35) Neyman, K. M.; Ruzankin, S. Ph.; Röscher, N. *Chem. Phys. Lett.* **1995**, *246*, 546.
- (36) Boys, S. F.; Bernardi, F. *Mol. Phys.* **1970**, *19*, 553.
- (37) Nasluzov, V. A.; Röscher, N. *Chem. Phys.* **1996**, *210*, 413.
- (38) Pacchioni, G.; Bagus, P. S.; Nelin, C. J.; Philpott, M. R. *Int. J. Quantum Chem.* **1990**, *38*, 675.
- (39) Bagus, P. S.; Pacchioni, G.; Nelin, C. J. In *Quantum-Chemistry: Basic Aspects, Actual Trends*; Carbo, R., Ed.; Studies in Physical and Theoretical Chemistry; Elsevier: Amsterdam, 1989; Vol. 62, p 475.
- (40) Perdew, J. P. *Phys. Rev. B* **1986**, *33*, 8822.
- (41) Pacchioni, G.; Röscher, N. *Acc. Chem. Res.* **1995**, *28*, 390.
- (42) Moore, C. E. *Atomic Energy Levels*; Natl. Bur. Stand. U.S. Circ. No. 467; GPO: Washington, DC, 1952.
- (43) Pyykkö, P. *Chem. Rev.* **1988**, *88*, 563.
- (44) Chung, S.-C.; Krüger, S.; Pacchioni, G.; Röscher, N. *J. Chem. Phys.* **1995**, *102*, 3695.
- (45) Birkenheuer, U.; Röscher, N.; Boettger, J. C. J. *Chem. Phys.* **1994**, *100*, 6826.
- (46) Campbell, C. T. J. *Chem. Soc., Faraday Trans.* **1996**, *92*, 1435.
- (47) Madey, T. E.; Diebold, V.; Pan, J. M. In *Adsorption on Ordered Surface of Ionic Solids and Thin Films*; Freund, H.-J., Umbach, E., Eds.; Springer: Berlin, 1993; p 147.
- (48) *CRC Handbook of Chemistry and Physics*; CRC: Palm Beach, 1993.
- (49) Zdesis, A. D.; Kunz, A. B. *Phys. Rev. B* **1985**, *32*, 6358.
- (50) Rao, F.; Wu, R.; Freeman, A. *Phys. Rev. B* **1995**, *51*, 10052.